2021

A Low-Cost, Wireless, Multi-Channel Deep Brain Stimulation System for Rodents

F. N. U. Tala
Boise State University

Jordan Leiber
Lafayette College

Hayden Fisher
Lafayette College

Naga Spandana Muppaneni
Lafayette College

Benjamin C. Johnson
Boise State University

 https://doi.org/10.1109/EMBC46164.2021.9629826

A Low-Cost, Wireless, Multi-Channel Deep Brain Stimulation System for Rodents

FNU Tala[1], Jordan Leiber[2], Hayden Fisher[2], Naga Spandana Muppaneni[2], and Benjamin C. Johnson[1]

***Abstract*— We present a small (43mm x 24mm x 15mm), off-the-shelf wireless neurostimulator for rodent deep brain stimulation research. Our device enables researchers to wirelessly configure stimulator settings, such as amplitude, pulse width, channel selection, and frequency, via a phone app. The system uses impedance-independent current-mode stimulation and steers current to a selected channel. In addition to monophasic and biphasic stimulation, the system also supports arbitrary waveform stimulation using pre-stored lookup tables. The system uses a configurable grounding phase to clear residual charge and a stimulation compliance monitor to ensure safe operation. The compliance monitor wirelessly reports the current during stimulation, the amount of passive recharge current, and the DC voltage of the electrode interface. The 400mAh battery is easy to replace and can go over 40 hours between charges. The system can be built for less than $50 using easy-to-source components to support inexpensive, highly-parallel research applications.**

***Keyword*— Bluetooth Low Energy (BLE); Full-feature stimulation; Multi-channel; Arbitrary Stimulation; Deep Brain Stimulation**

I. Introduction

Deep brain stimulation (DBS) is a 25-year-old FDA-approved treatment for advanced Parkinson's disease and is promising for many other neurological disorders. Despite remarkable clinical success in the symptomatic treatment of Parkinson's disease, the mechanism of action for DBS is still unclear. Neurotoxins that selectively destroy dopaminergic neurons can be used to create animal models that successfully recapitulate the hallmark motor symptoms Parkinson's disease [1]. As with Parkinson's, DBS ameliorates the motor symptoms in these animal models as well, meaning the animal models can be used to study the mechanisms of DBS and investigate new treatments for DBS therapy.

Clinical DBS devices are far too large for rodent use and are optimized for ultra-low power chronic use, meaning they lack the feature flexibility to explore new therapeutic stimulation paradigms. Most commercially available research systems are rack-mounted and require a tether. While a commutator can be used to permit less constrained movement to evaluate open-field locomotor activity, the equipment is still expensive, hindering highly parallel experimentation. Therefore, in this paper we present a DBS system that is small enough for rodent use and emulates bilateral, clinically-relevant electrical stimulation. The system is capable of arbitrary stimulation for therapeutic exploration in addition to fully-customizable mono- and biphasic stimulation [2]. The system uses wireless Bluetooth Low Energy (BLE) communication for untethered movement and on-the-fly (OTF) update of stimulation parameters for adaptive DBS study. The system also uses a compliance monitor to verify stimulation pulses in situ and monitor the electrode interface for charge build-up, which can damage tissue. While many ASIC (application specific integrated circuit) implementations boast a powerful stimulation feature set [3], [4], they are not widely available for neuroscience research. Therefore, the presented system is low-cost, reusable, and comprised of readily available off-the-shelf components for widespread adoption by research labs. The system can be programmed easily via OTF updates to experiment various therapeutic stimulation protocols. With both stimulator and recording front-end, this system can perform closed-loop neuromodulation: stimulation parameters changes based on feedback from the recording signals.

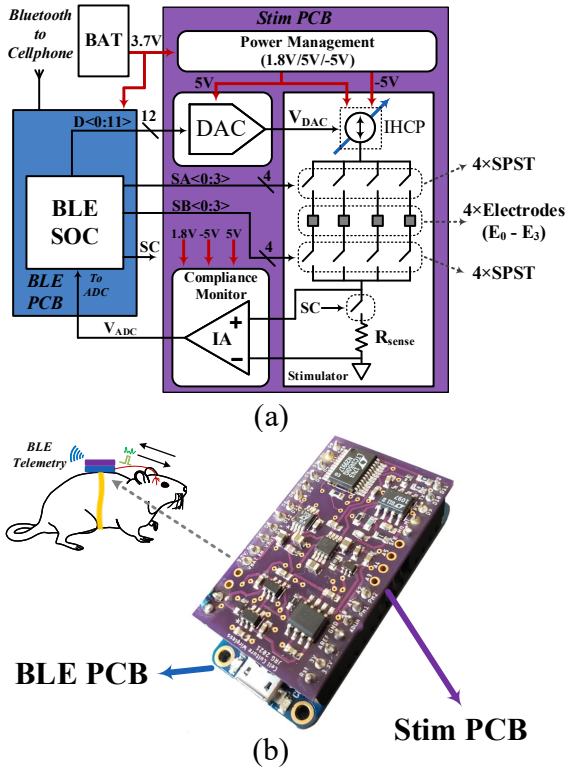

Fig. 1. (a) System architecture and (b) 3D model of stacked Stim PCB (purple) and BLE PCB (blue).

[1]FNU Tala and Benjamin C. Johnson are with the Dept. of Electrical and Computer Engineering, Boise State University, Boise, ID USA bcjohnson@boisestate.edu

[2]Jordan Leiber, Hayden Fisher, and Naga Spandana Muppaneni are with the Dept. of Electrical and Computer Engineering, Lafayette College, Easton, PA USA.

This work was made possible by an Institutional Development Award (IDeA) from the National Institute of General Medical Sciences of the National Institutes of Health under Grant P20GM103408.

II. System Description

A. System Architecture

The implemented system architecture and its 3D model are shown in Fig. 1. It consists of a printed-circuit board (PCB) for the stimulator subsystem and a commercially available PCB with BLE system on a chip (SoC; Feather nRF52840 Express) that stack. The stimulator system is comprised of a 12-bit digital-to-analog converter (DAC; LTC1450), an improved Howland current pump (IHCP) [5], and two 4-channel single pole single throw switches (ADG452). The output current range is ±81.92µA designed for 75-µm platinum-iridium (PtIr) microstimulation electrodes to limit the voltage across electrode's double-layer within a safe electrochemical window. Users can adjust the stimulation current range by replacement of surface mount (SMD) resistors on the stimulator PCB. Using the built-in memory of the microcontroller unit (MCU), one can avoid extra hardware or circuits (e.g., 3^{rd}-order low-pass filtering of square waves) required to generate sinusoidal waveforms or any other arbitrary waveforms. The compliance monitor is built around an instrumentation amplifier (IA; IN818), which senses the current flow by amplifying the voltage across a small sensing resistor and then drives an analog-to-digital converter (ADC) of BLE SoC for wireless transmission.

B. Stimulator and Current Source

The stimulator system in Fig. 1a uses BLE SoC to wirelessly communicate between PC/Mobile interface and stimulation circuitry. Users can initialize the transmission of the stimulation parameters through the universal asynchronous receiver-transmitter (UART) transmission services on a phone App (e.g., Bluefruit Connect), where stimulation timing and amplitude parameters are sent via a list of comma separated values.

The IHCP shown in Fig. 1a is the main component for the stimulator. It can behave as either current sink or source depending on the input DAC code (12-bit, 0 to 4095, mid-value is zero current). The operational amplifier (op-amp; LT1097) used in IHCP has a rail-to-rail voltage of ±5V, which sets the voltage compliance of electrical stimulation. This can system can support ±10V, but, due to the electrode impedance and limitation of the electrochemical window, a ±5V compliance voltage is sufficient for our application. By changing the resistor values of the IHCP, the maximum output current range can be extended proportionally according to research needs. The output current amplitude is controllable through a 12-bit DAC, and the current resolution is 40nA under ±81.92µA range. The current step scales according to the maximum current range selected.

The compliance monitor is a fixed gain (200V/V) IA with a 1.8V offset added to the reference. The 1.8V offset centers the voltage output of IA to match the ADC input range. The compliance monitor senses the voltage across the sensing resistor, which is a small resistor (100Ω) in series with the load. The sensed voltage is then fed to the ADC input of the BLE SoC, digitized, and then sent over the wireless link. The IA has an input bias current less than ±500pA.

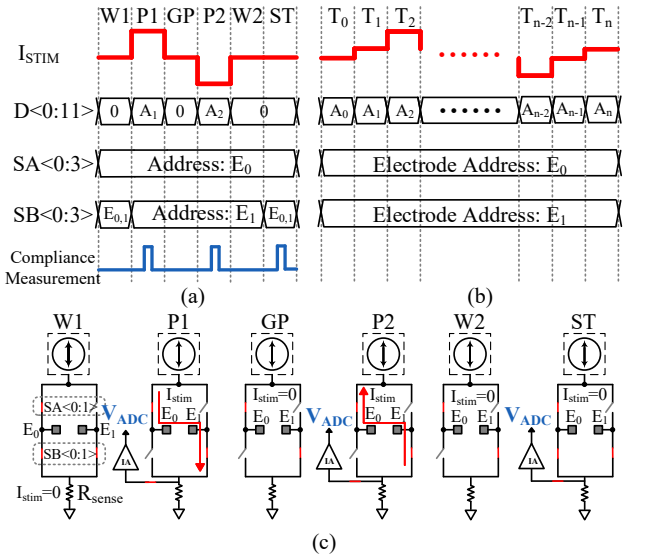

Fig. 2. (a) Example timing for biphasic, (b) arbitrary using lookup table update and (c) equivalent circuit concept operation of biphasic

C. Digital Timing Control

Fig. 2a shows the digital timing control diagram for a standard biphasic pulse stimulation while Fig. 2c shows the equivalent circuit. Each biphasic pulse has 6 independently programmable states: Wait (W1), Phase 1 (P1), interphase gap (GP), Phase 2 (P2), Wait 2 (W2), and shorting-time (ST). The timing resolution for each phase is 1µs, and the delay time period for each phase is fully configurable through the wireless BLE user interface. Note that monophasic stimulation is achieved by setting the width of P2 to zero. The stimulation repetition rate is governed by W1. The digital timing control was configured to let the stimulator operate in the current steering mode, so at any moment output current has a DC pass to flow. This eliminates any transient current spikes associated with load switching. Transient current spikes result in large errors for nominally small current amplitudes or narrow pulse widths. W1, W2, and GP are periods when stimulation current is zero across the load and any leakage or offset currents are shunted to ground in lieu of several blocking capacitors. During P1 and P2, the current flow direction is reversed from cathodic to anodic to perform the biphasic pulse. The amplitude for each phase is fully adjustable so even unbalanced biphasic pulses can be generated. To verify successful stimulation and to check whether the current source is compliant, the compliance monitor measures current flow in the middle of the P1 and P2. During ST, both electrode channels are tied to the ground to allow the discharge of the electrochemical interface. Current flow is measured during ST as well to determine the magnitude of the passive charge balancing current. Note that the SC switch can be open so the IA can measure the offset voltage of the stimulator. These real-time monitoring features give users a clear validation of the stimulation protocol.

Fig. 2b shows the digital timing control of any arbitrary waveform. During this mode, both channels are addressed so the current amplitude is completely controlled by updating

the DAC input code with a pre-populated lookup table, which in turn will control the IHCP current amplitude. A MATLAB script is used to generate the lookup table for any applications (shapes and number of points). Compliance monitoring is supported in this mode but must be specified by the user. The timing resolution is 1µs for both biphasic and arbitrary modes.

III. Results

A. System Transfer Function

The measured output current transfer function is shown in Fig. 3. The DAC code is swept from 0 to 4095 for the 12-bit DAC. The voltage is measured across a 50kΩ load terminated to the ground and the current is calculated by dividing the measured voltage with resistor load value.

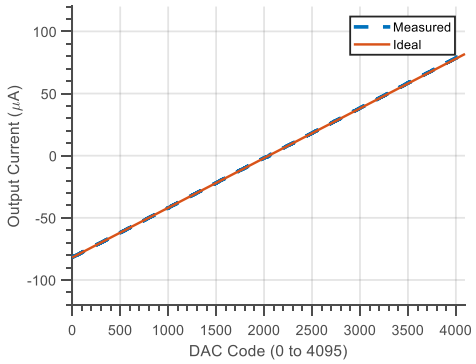

Fig. 3. Measured current source transfer function compared to ideal transfer function.

B. Waveform Generation

To demonstrate the programmability of the system and its arbitrary waveform generation capabilities, we measured the voltage across a 10kΩ load. Fig. 4a shows the biphasic waveform mode with rectangular current pulses. Each stimulation state and the amplitude for each pulses is independently programmable over the wireless interface. Fig. 4b demonstrates the arbitrary waveform mode where sine waves are generated using a 64-point lookup table. Users can customize the timing and amplitude which scales the arbitrary waveform. High-resolution sine waves are generated by using the points of 1/4 cycle and then mirroring the points appropriately to generate a full sinusoid. Fig. 5 shows additional examples of arbitrary stimulation waveforms for therapeutic investigations.

C. Charge-Balancing in RC Model

Biphasic stimulation requires precise charge balancing between the phases to ensure safety (typically <1% mismatch). Such precision requires careful calibration, component selection, and low timing jitter. Even with high-performance stimulation electronics, nonlinearities of the electrode interface can make this difficult to achieve with large amplitude stimulation or a long interphase gap. Therefore, we incorporated a shorting phase to clear residual charge and a DC interface monitor to ensure safety. This relaxes the matching requirements of precision resistors and offset calibration.

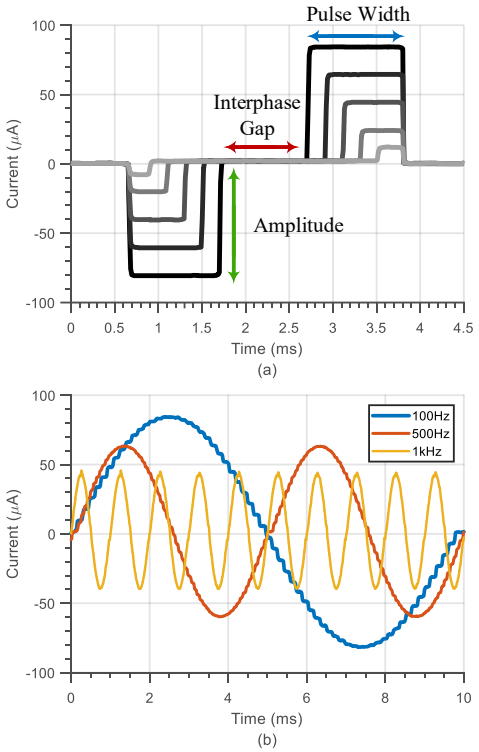

Fig. 4. (a) Biphasic timing and amplitude can be fully-customized. (b) Sinewave generation via scaleable lookup tables.

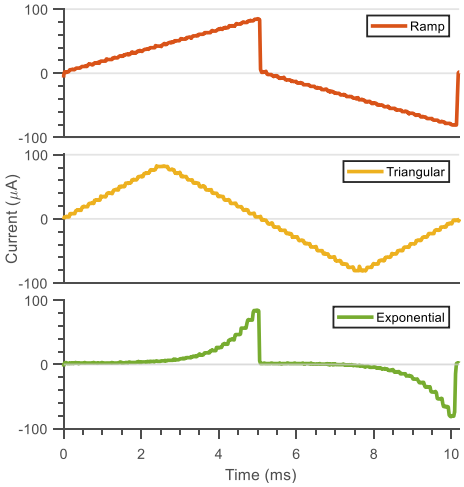

Fig. 5. Arbitrary waveform stimulation with ramp, triangular and exponential waveforms using pre-computed lookup tables.

To demonstrate the charge-balancing ability of the system, we injected an intentionally mismatched biphasic pulse into an RC Randles cell model of the electrode-electrolyte interface. The RC is a simplified model for a circular Pt-Ir electrode with a diameter of 175µm as a model of electrochemical interface, where the spreading resistance, R_S, was 10kΩ and the double-layer capacitance, C_{DL}, was 10nF. Fig. 6 shows the measured voltage across the electrode during the stimulation cycle. Each phase is 250µs long and the P1 and P2 amplitudes are 81µA and 82µA, respectively.

During P1, the current flowed through the electrode model, dropping the voltage by $-I_{stim} \cdot R_S$ at the beginning of P1 and then charging C_{DL} with a constant current. During GP, the current flow was zero so the voltage jumped down by I_{stim}

TABLE I

COMPARISON OF STATE-OF-THE-ART NEUROMODULATION RESEARCH DEVICES

	2016 [6]	2015 [7]	2017 [4]	2019 [5]	2019 [8]	2020 [9]	This Work
Wireless Telemetry	No	No	No	No[a]	No	BLE	BLE
Off-the-self	Yes	Yes	No	Yes	Yes	No	Yes
Arbitrary Stimulation	No	No	Yes	No	No	No	Yes
Addressable Channels	2	2	8	2	2	64	4
Safety Monitoring	No	No	No	No	No	No	Yes
I_{max} (µA)	2036	100-400	1000	150	5000	5000	±81.92 [b]
Current Resolution	10b (nonlinear)	100µA	4µA	NA	8b (20µA)	6b (20µA)	12b (40nA)
Timing Resolution (µs)	0.5	2	20	95 (fixed)	1	16	1
V_{max} (V)	17	12	±20	±7	±18	12	±5
f_{stim} (HZ)	10-300	200 (fixed)	NA	130 (fixed)	0-2k	15-255	0-50k (variable)
Battery/Power	(3×) Zn:air	(4×) Zn:air	Benchtop	150mAh Li-Po	250mAh Li-Po	500mAh Li-Po	400mAh Zn:air
Dimension (mm^3)	30×14×24	13×13	Benchtop	36×20×12	46×36	36×33×15	43×24×15
Weight (g)	13.8	2.3	NA	10	16.8	18	15
Lifetime	6d	14d	NA	31d	12d	11h (172mW)	40h (36mW)
q-Balancing Method	None	Elec. Shorting	None	None	None	Elec. Shorting	Elec. Shorting
Animal Model	Rodent	Rodent	Rodent	Rodent	Rodent	NHP	Rodent

[a] Wireless charging capability. [b] Adjustable by replacing SMD resistors.

$\cdot R_S$ from the negative peak. During P2, current polarity was reversed, which discharged C_{DL} with a constant rate. If the phases were perfectly balanced, the voltage potential at W2 would be zero. For this measurement, the phase mismatch results in an incomplete discharge of C_{DL} as shown in Fig. 6. During ST, both channels are shorted to the ground in order to eliminate the voltage offset stored in C_{DL}.

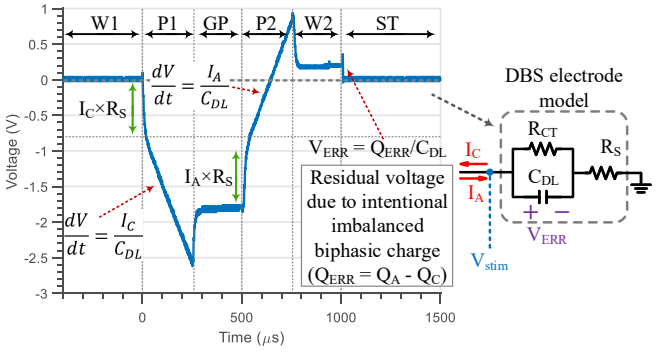

Fig. 6. Measurement of electrode shorting to clear residual charge.

IV. CONCLUSION

Table I shows a comparison of state-of-the-art DBS neuromodulation systems. Compared to the presented work, most other work has optimized battery-life over wireless telemetry and stimulation waveform flexibility. While long battery life is preferable for chronic experiments, the lack of monitoring capabilities is a serious drawback as experimental errors, such as a dead battery or an open circuit, may go undetected. As such, most of the current draw (7.65mA) in our system was to power the BLE SoC. We selected a 400mAh battery so that the system could go over 40 hours between swapping batteries. This work presented a low-cost, multi-channel DBS system for rodent neuroscientific research. With the on-board BLE SoC, users can specify the stimulation parameters using a phone app wirelessly. The system's ability to generate arbitrary stimuli is comparable to benchtop systems [10] or ASICs [4]. By utilizing only commercially available components and economical PCBs, the presented system can be built for less than $50.

REFERENCES

[1] K. Tieu, "A guide to neurotoxic animal models of Parkinson's disease," *Cold Spring Harbor Perspectives in Medicine*, vol. 1, sep 2011.

[2] T. J. Foutz and C. C. McIntyre, "Evaluation of novel stimulus waveforms for deep brain stimulation," *Journal of Neural Engineering*, vol. 7, p. 066008, dec 2010.

[3] B. C. Johnson, S. Gambini, I. Izyumin, A. Moin, A. Zhou, G. Alexandrov, S. R. Santacruz, J. M. Rabaey, J. M. Carmena, and R. Muller, "An implantable 700μW 64-channel neuromodulation IC for simultaneous recording and stimulation with rapid artifact recovery," in *IEEE Symposium on VLSI Circuits, Digest of Technical Papers*, pp. C48–C49, Institute of Electrical and Electronics Engineers Inc., aug 2017.

[4] J. Castelli, F. Kolbl, R. Siu, G. N'Kaoua, Y. Bornat, A. Mangalore, B. Hillen, J. J. Abbas, S. Renaud, R. Jung, and N. Lewis, "An IC-based controllable stimulator for respiratory muscle stimulation investigations," in *Proceedings of the Annual International Conference of the IEEE Engineering in Medicine and Biology Society, EMBS*, pp. 1970–1973, Institute of Electrical and Electronics Engineers Inc., sep 2017.

[5] M. Schulz, J. Zschabitz, E. Reese, R. Hadart, C. Winteri, and R. Thewes, "A Rechargeable Battery-Driven, More than 4 Weeks Runtime, Biphasic Bilateral DBS Unit for Rodents," in *Proceedings - 2019 8th International Workshop on Advances in Sensors and Interfaces, IWASI 2019*, pp. 15–19, IEEE, jun 2019.

[6] F. Kölbl, G. N'Kaoua, F. Naudet, F. Berthier, E. Faggiani, S. Renaud, A. Benazzouz, and N. Lewis, "An Embedded Deep Brain Stimulator for Biphasic Chronic Experiments in Freely Moving Rodents," *IEEE Transactions on Biomedical Circuits and Systems*, vol. 10, pp. 72–84, feb 2016.

[7] A. I. Acosta, M. S. Noor, Z. H. Kiss, and K. Murari, "A lightweight discrete biphasic current stimulator for rodent deep brain stimulation," in *IEEE Biomedical Circuits and Systems Conference: Engineering for Healthy Minds and Able Bodies, BioCAS 2015 - Proceedings*, pp. 1–4, Institute of Electrical and Electronics Engineers Inc., dec 2015.

[8] D. Guo, S. Mai, C. Zhang, X. Fu, and Y. Zhao, "A Low-cost Electrical System with High Compliance of Supply Voltage for Deep Brain Stimulation on Rats," in *Proceedings - APCCAS 2019: 2019 IEEE Asia Pacific Conference on Circuits and Systems: Innovative CAS Towards Sustainable Energy and Technology Disruption*, pp. 133–136, Institute of Electrical and Electronics Engineers Inc., nov 2019.

[9] A. Zhou, S. R. Santacruz, B. C. Johnson, G. Alexandrov, A. Moin, F. L. Burghardt, J. M. Rabaey, J. M. Carmena, and R. Muller, "A wireless and artefact-free 128-channel neuromodulation device for closed-loop stimulation and recording in non-human primates," *Nature Biomedical Engineering*, vol. 3, no. 1, pp. 15–26, 2019.

[10] F. Tala and B. C. Johnson, "MEDUSA: A low-cost, 16-channel neuromodulation platform with arbitrary waveform generation," *Electronics (Switzerland)*, vol. 9, p. 812, may 2020.